J. Phys. D: Appl. Phys. 27 (1994) 2547–2555. Printed in the UK

Electrical and spatial correlations between direct current pre-breakdown electron emission characteristics and subsequent breakdown events

N S Xu and R V Latham

Department of Electronic Engineering and Applied Physics, Aston University, Birmingham B4 7ET, UK

Received 27 May 1994, in final form 13 September 1994

Abstract. An experimental study has established that correlations exist between the pre-breakdown electron emission characteristics and the associated breakdown events that occur in a high-voltage vacuum gap formed by OFHC Cu electrodes. A tin-oxide-coated 'transparent anode' imaging technique was employed to display the spatial distribution of pre-breakdown emission sites and the locations of subsequent direct current breakdown events. By using a real-time video recording technique, it has been possible to demonstrate that a correlation exists between the spatial location of a pre-breakdown emission site and a subsequent direct current breakdown event, and to investigate the time evolution of the two processes. The pre-breakdown electrical characteristics of emission sites, namely their switch-on fields and β values, are also correlated with the threshold field for direct current breakdown. A new breakdown-initiating mechanism is considered, and subsequently used to explain the findings that emerged from this study.

1. Introduction

Traditional theories describing the breakdown mechanism of a high-voltage (HV) gap have been based on the metallic-microprotrusion model (Latham 1981, Schwirzke 1991, Mesyates and Proskurovsky 1989, Lafferty 1966). According to these theories, a vacuum discharge can be either cathode-initiated or anode-initiated, dependent typically upon the specific operational conditions and the configurations of the HV gap. The pre-requisite for the assumed initiating processes is a thermal instability caused by a pre-breakdown electron emission current. In the case of cathode-initiated breakdown, the electron current generates Joule heating in a field-emitting metallic microprotrusion, whilst in the case of anode-initiated breakdown, it is the thermal instability of an anode 'hot spot' bombarded by the pre-breakdown electron current from an isolated cathode emission site that is involved. However, it is now well established that the electron emission responsible for the pre-breakdown current of a HV vacuum gap comes from *non-metallic* particulate microstructures on the surface of the cathode (Allen and Latham 1978, Athwal and Latham 1981, Bayliss and Latham 1986, Niedermann 1986, Latham and Xu 1991, Latham 1981). This, therefore, raises important questions about the general validity of the traditional breakdown theories, and the associated need to investigate experimentally the detailed nature of the vacuum breakdown process.

An early study by Latham *et al* (1986) pioneered the use of the 'transparent anode' technique to investigate whether a spatial correlation exists between a pre-breakdown emission site (PES) and a primary breakdown arc in both a high-voltage (HV) vacuum gap and one employing high-pressure (HP) gas. By viewing either type of high-voltage gap through this transparent anode, a map of the spatial locations of the PESs was recorded by photographing the positions of the luminous 'anode spots' produced by the impinging high-energy electrons. By using the camera in an 'open shutter' mode, the spatial locations of the subsequent vacuum and high-pressure SF_6 gas breakdown events (HPBE) were also recorded. Thus, by superimposing the pre-breakdown and breakdown images, it was possible to establish that a direct spatial correlation exists between (i) a vacuum PES and the first vacuum arc (Latham 1988), and (ii) a vacuum PES and a HPBE (Latham *et al* 1986). However, in both cases, the spatial resolution was limited by the 'open-shutter' photographic recording technique.

In the present study, the transparent anode imaging technique has been refined by incorporating a modern video camera recording method. This system has three

0022-3727/94/122547+09$19.50

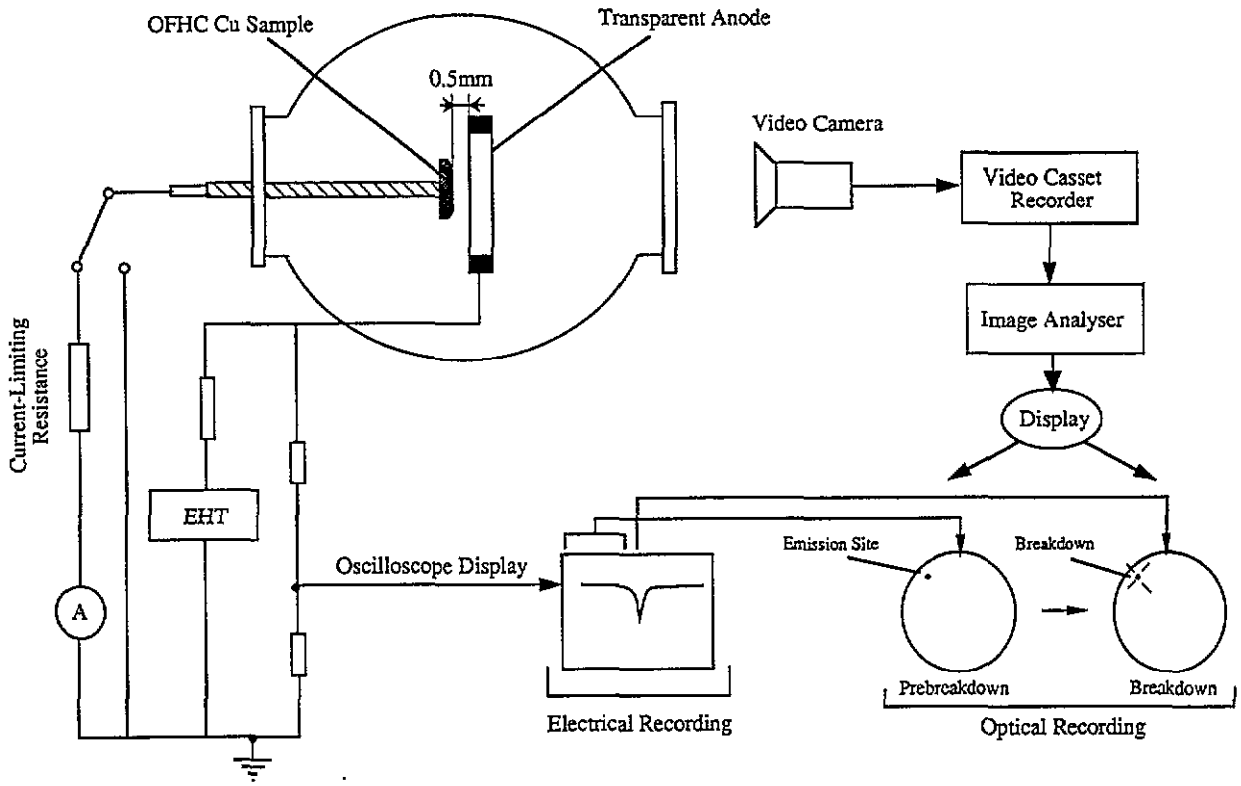

Figure 1. The lay-out of the experimental system used for the present study, showing the combination of transparent anode imaging and real-time video camera recording techniques for studying spatial and electrical correlations between pre-breakdown and breakdown processes.

advantages over the previous 'open shutter' photographic approach: (i) it makes possible continuous video filming of any optical events in the high-voltage gap; (ii) it reduces the framing speed to 40 ms per frame from the minimum of 2 min per frame of the early method; and (iii) it has a high spatial resolution, about 30 μm, which is only limited by the horizontal resolution of the video camera used in this study. This paper reports on how this new system has been adapted to determine (i) whether or not a correlation exists between the characteristics of individual pre-breakdown emission sites and their probability of initiating a primary DCBE event under vacuum conditions, and (ii) the detailed nature of a vacuum DC breakdown process, including the nature of the resultant effects of the primary breakdown discharge on the subsequent behaviour of the gap.

2. Experimental

2.1. The system

Figure 1 is a schematic illustration of the experimental set-up. This is based upon an UHV chamber (< 10^{-9} mbar) containing a plane-parallel test gap having a spacing of 0.5 mm that is formed between a 30 mm diameter transparent anode and a 15 mm diameter Cu cathode. The transparent anode is made from a glass substrate coated with conducting tin oxide. Thus, electrons emitted from PESs will be accelerated by the gap field, and on bombarding the tin oxide layer generate visible light. In practice, one obtains a distribution of highly localized 'light spots', which correspond to a 'map' of the emission sites. When a breakdown discharge occurs, electrons emitted from the cathode spot can cause strong transition radiation to be emitted from the anode; indeed, this light may be so bright that it is often not possible to identify that generated in the cathode spot (Latham 1988).

To overcome this difficulty, the present study has made a significant step forward by employing a video camera (Parasonic WV-F15, horizontal resolution more than 460 lines) technique to reduce the framing time. It has also enabled recording of real-time sequences of both variation in total emission current from the cathode surface with gap voltage, and the evolution of subsequent breakdown events. To complement these recordings, an oscilloscope (HAMEG model 208) is used to monitor the time-profile of the collapsing gap voltage. In addition, an image analyser, 'ArcImage 5' developed by Foster Findlay Associates, is employed for detailed analysis of each frame of the recorded video sequences. Thus, an interesting frame can be grabbed and stored in a computer memory. Such an image can then be processed to have better contrast, and so on. For the present study, this facility proved particularly useful in the following applications: (i) capturing and displaying two consecutive frames showing the transition process from a pre-breakdown emission site to a breakdown arc centre (see figure 4 later), and (ii) providing the

Table 1. Parameters for the various samples. Y=yes, N=no.

Parameter	Sample 1	2	3	4	5	6	7	8	9	10
Switching-on field (MV m^{-1})	12	12	14	23.3	20.4	16.8	17.2	28.7	14.8	19.2
Breakdown field (MV m^{-1})	10.9	17.8	8.8	15.6	20.7	15.2	14	18.4	10.2	23.7
β	399	173	661	242	171	181	201	198	578	158
Correlation	Y	Y	Y	Y	N	Y	Y	Y	N	Y

opportunity to print out the enhanced images directly from a laser printer.

It will also be seen from figure 1 that a 100 MΩ current-limiting resistance is connected in series with the EHT power supply in order to isolate it electrically from the HV gap, and thus prevent the supply switching off when the gap breaks down. Consequently, the gap is automatically re-charged following a DCBE event. This arrangement also has the advantage of limiting the current supply to the gap, so that a breakdown discharge cannot evolve into a continuing vacuum arc. However, as monitored on the oscilloscope, it does not prevent the gap voltage temporarily collapsing to zero during such an event.

2.2. Procedures

In preparation for a measurement, the high-field surface of the test Cu cathode is mechanically polished and cleaned in an ultrasonic spirit bath. It is then mounted in the experimental chamber and carefully adjusted to form a 0.5 mm plane-parallel gap between the transparent anode and the cathode. Having achieved an operating pressure of $\leqslant 10^{-9}$ mbar, it is now necessary to increase the field applied to the virgin specimen very slowly until its 'first generation' emission sites are 'switched on' to establish a reversible pre-breakdown current. Typically, the initial switch-on field is in the range 10–20 MV m^{-1}, after which the specimen exhibits a stable I–V characteristic over a decade change in field. The typical form of switching-on process and the subsequent reversible pre-breakdown current characteristic are illustrated in figure 2. A particularly important practical feature of this behaviour is the initial hysteresis effect exhibited by the pre-breakdown current.

For a breakdown measurement, the cathode is directly connected to earth, so that possible damage to the picoameter (A in figure 1) is avoided. In order to create a breakdown of the test gap, the applied field needs to be slowly increased to a value that is considerably higher than that used to measure the stable and reversible pre-breakdown I–V characteristic. During this procedure, the oscilloscope is set to an external trigger mode so that its electron beam scan is initiated by a negative-going leading edge of a pulse. A sudden drop of gap voltage, as shown on the oscilloscope, signals the occurrence of a breakdown discharge. With this arrangement, the oscilloscope records the gap voltage profile from the time this initial breakdown starts to the end of an interval determined by the choice of oscilloscope time setting.

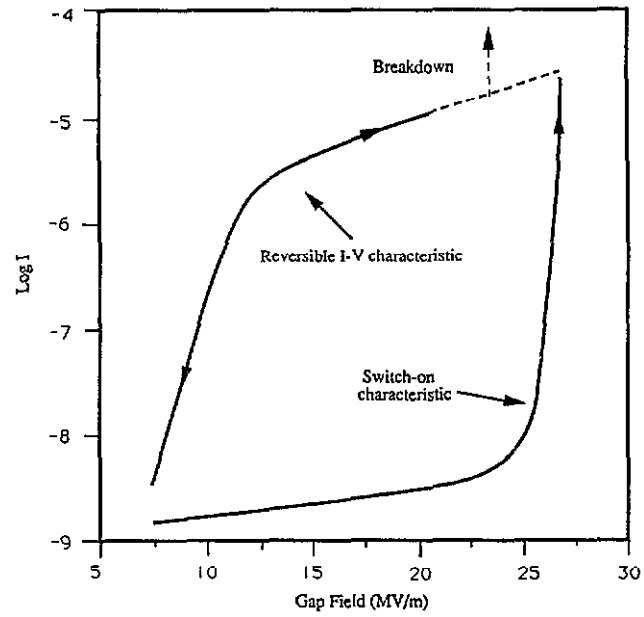

Figure 2. A schematic representation of the typical I–V characteristic of pre-breakdown emission sites. A reversible current may be measured after an emission site is 'switched on'; however, a breakdown event may occur before the switching-on field is reached during the re-cycling process.

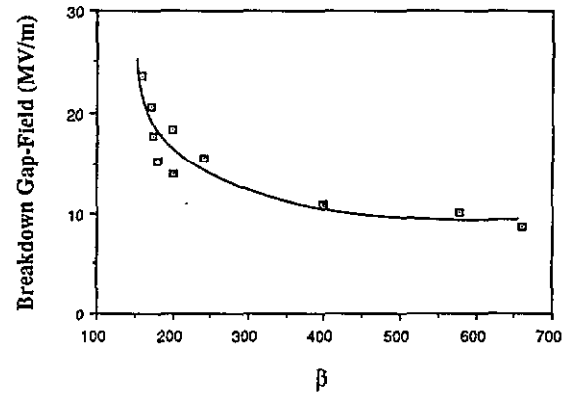

Figure 3. Showing how the macroscopic breakdown field (or breakdown gap field F_b) decreases from low-β sites to high-β sites.

Concurrent with these electrical measurements, the

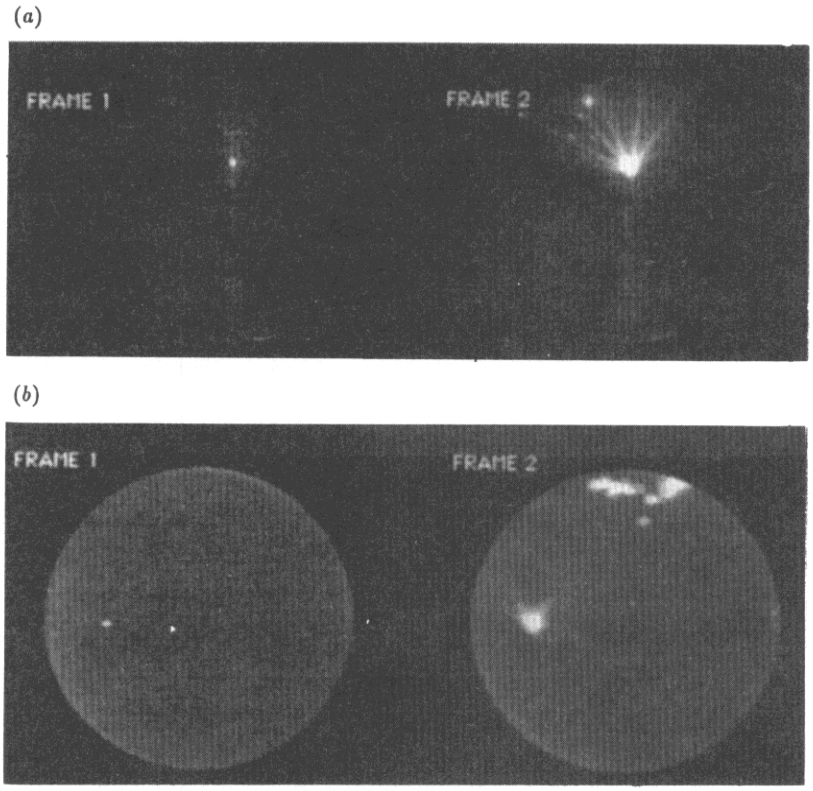

Figure 4. Examples of type I and type II breakdown processes. In both cases, two consecutive video frames show how a pre-breakdown emission site in frame 1 develops into a subsequent breakdown event in frame 2.

video camera system makes a continuous recording of any optical activity that occurs in the gap, thus making it possible to correlate the optical and electrical characteristics.

2.3. Findings

2.3.1. Dependence of breakdown field on prebreakdown I–V characteristics. The first set of findings is derived from measurements of the 'total' I–V gap characteristics and the associated Fowler–Nordheim plots of the ten samples used for this study. Thus, referring to the tabulated data of β values, switching-on and breakdown fields presented in table 1, the following two general conclusions can be drawn:

(i) as shown in figure 3, the higher β, the lower the breakdown field, and

(ii) the breakdown field of the primary discharge is usually (seven cases out of ten) lower than the initial switching-on field of the corresponding pre-breakdown emission site.

2.3.2. Spatial correlation between pre-breakdown emission sites and subsequent breakdown discharges. In order to establish whether such a correlation exists, it is necessary to examine frame by frame the transient video sequence showing evolution of the spatial distributions of the pre-breakdown emission sites into subsequent breakdown events. The first important finding to emerge from this investigation is shown in sequences (a) and (b) of figure 4, which present two optical images obtained from two independent sequences of video frames (the framing time is 40 ms). Frame 1 of both (a) and (b) displays the spatial distribution of PESs captured just before breakdown, while frame 2 of (a) and (b) has recorded a 'map' of the locations of subsequent discharges constituting breakdown of the gap. From comparison of these images, it can be seen that there are two types of process: type 1, as shown in sequence (a), has only one subsequent breakdown discharge during the framing time of 40 ms, whilst type II, as shown by sequence (b), have five discharge centres occurring in the same 40 ms period of time. This therefore highlights an important characteristic of many of the breakdown processes observed in this study, namely a 'primary' event appears to trigger a number of 'secondary' events.

More importantly, it can also be seen from figure 4 that the location of the breakdown event shown in frame 2 of sequence (a) is at the same position as the PES shown in frame 1. Such a spatial correlation also exists in the event shown in sequence (b). In a systematic study of ten samples, eight of them suffered breakdown events that exhibited clear spatial correlations with PESs, whilst one of the other two exhibited a breakdown event that was located very near to a previous PES. Thus, it was in only one case out of ten that the breakdown discharge did not clearly correlate with a precursor PES.

2.3.3. Associated electrical observations. As mentioned above, and also shown in sequence (*b*) of figure 4, a 'primary' breakdown generally results in a group of discharges in the gap. It was noticed from this observation that the spatial evolution of these discharges is not predictable, and can spread out over a large area of the gap. However, with the current video system, it is impossible to resolve in terms of time whether such a group of discharges occurs in sequence or simultaneously. However, as we will see shortly, some relevant information can be derived from a complementary study of the time profile of the collapsing gap voltage associated with the optical events shown in figure 4.

Thus, figure 5(*a*) is a typical example showing how the gap voltage profile varies within a period of about 250 ms, where a collapse of the gap voltage appears as a downward-pointing spike. As described in section 2.3.2, this profile records a multiple gap breakdown event initiated by the 'primary' discharge. It can be seen from figure 5(*a*) that 24 such spikes are involved in the progressive collapse of the gap voltage, giving an averaged rate equal to approximately one spike per 10 ms. Accordingly, one can expect that the gap voltage will collapse around 4–5 times within a period of 40 ms, which is equal to the framing time of the video camera used in present study. This figure coincides with the number of discharge centres recorded in one video frame of a typical type II breakdown process.

To examine the time profile of the gap voltage in more detail, the scanning speed of the oscilloscope was increased to 5 ms per division to obtain the typical sequence shown in figure 5(*b*). From these two sequences, it is possible to make three important observations. Firstly, the leading edge of any one of the collapsing voltage spikes is very sharp, indicating that gap breakdown is a very fast process. Secondly, the gap voltage recovers relatively slowly, in about 3 ms, as is evident from the long tail of the voltage profile, and indeed as predicted by the *RC* time constant of the circuit. In fact, a gradual reduction in the recovery time was observed as the *RC* time constant was progressively decreased through charging the current limiting resistance from 80, 50 and 10 MΩ resistors, respectively. Thirdly, a second breakdown occurs after the gap voltage is re-established, although this does not necessarily start immediately after the gap voltage is re-established; typically the 'dwelling time' can be about 50 ms. This is a particularly significant finding, since it demonstrates that a previous breakdown discharge results in an irreversible change to the vacuum gap; in particular, it creates new electron emission centres in an area of the electrode that was previously emission-free. Furthermore, these new centres become unstable immediately after a gap field is re-established.

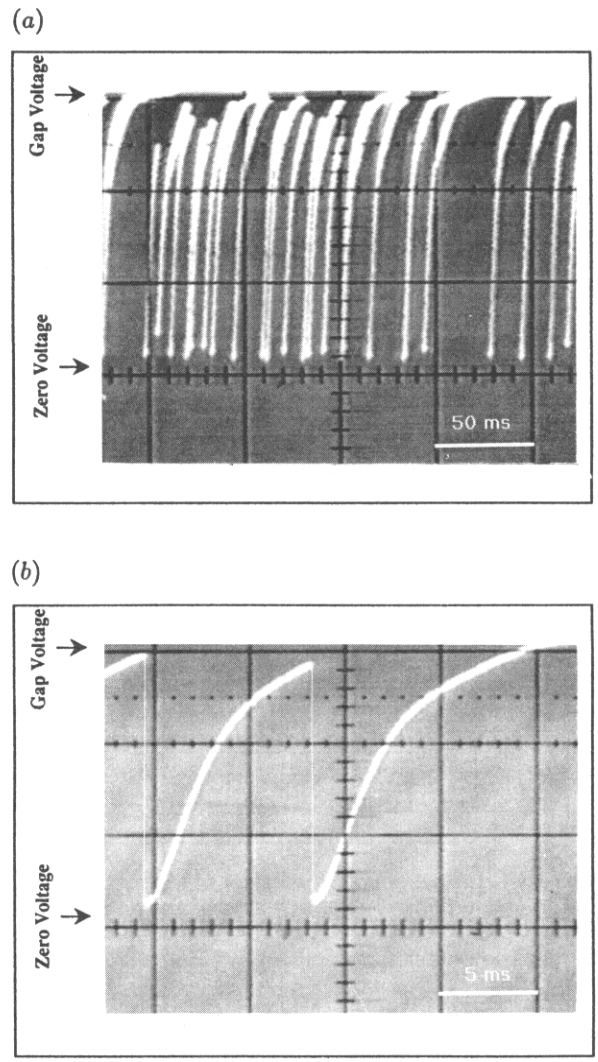

Figure 5. Oscilloscope traces showing (*a*) a typical sequence of collapsing voltage spikes recorded at a low scan speed and (*b*) the detailed shape of two such spikes recorded at a higher scan speed.

3. Discussion

The experimental results presented in the last section have established that a DC breakdown process is initiated at a DCPES, and that a 'primary' arc can trigger a sequence of 'secondary' discharge events. In addition, it has also been shown that there is an electrical correlation between the DC pre-breakdown characteristics and the threshold field of the DCBE. In the following, we shall present our understanding of the physical processes involved in a DCBE.

3.1. Micro-plasma generation at a metal–insulator surface structure

Most models (Schwirzke 1991, Mesyates and Proskurovsky 1989, Lafferty 1966) that have been proposed to explain the vacuum breakdown process assume the existence of metallic microprotrusion emitters on broad-area HV electrodes. However, as explained in the introduction, the available evidence indicates that the predominant sources of pre-breakdown currents result from a hot-electron emission process that is associated with isolated particulate non-metallic microstructures on an electrode surface (Latham 1981,

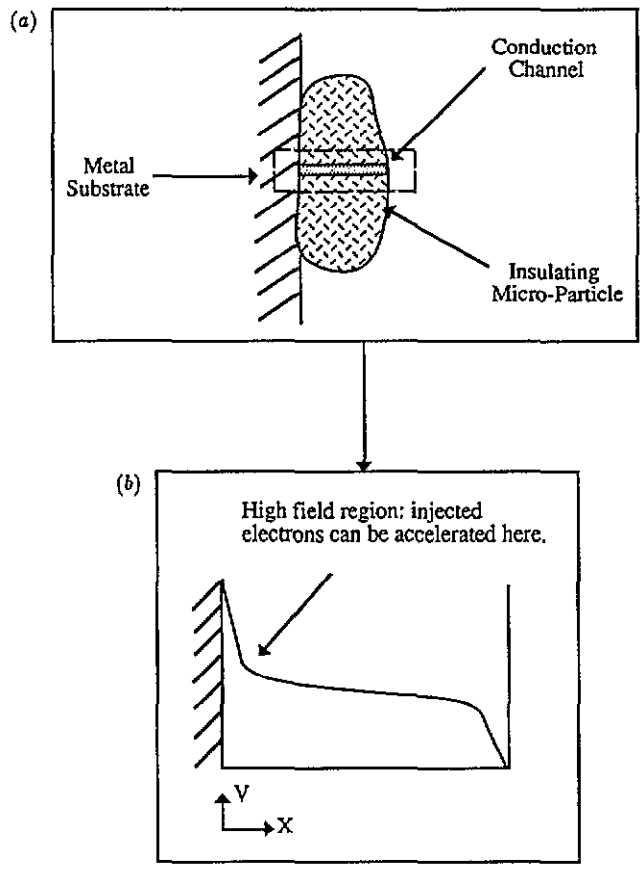

Figure 6. (*a*) A schematic illustration of the metal–insulator–vacuum micro-regime that is assumed to be responsible for the majority of pre-breakdown emission sites. (*b*) The potential distribution within a microchannel in its 'on' state.

Latham and Xu 1991, Bayliss and Latham 1986). In order therefore to explain the newly established spatial correlation, a revised qualitative model of the vacuum breakdown process will be developed in the following paragraphs based on this type of non-metallic emission regime.

Thus, referring to figure 6, it is assumed that an emission structure involves a metal–insulator–vacuum (MIV) micro-regime, which can relate to an insulating particle either resting on or embedded in the surface of a metallic electrode (Bayliss and Latham 1986, Athwal and Latham 1986, Niedermann 1986). It is further assumed that, as described in detail elsewhere (Bayliss and Latham 1986), an initial cycle of increasing external field causes electroforming of an electron conduction channel in the insulating medium. Subsequently, under the influence of the electric field penetrating the insulating medium, electrons can pass through this channel from the metallic substrate to the vacuum surface, there to be emitted in a quasi-temperature-assisted field emission manner (Bayliss and Latham 1986, Xu 1986).

To understand how a micro-plasma can be created in this type of conduction channel regime, we can refer to the early works of other authors (Ridley 1975, DiStefano and Shatzkes 1976, Solomon 1977), who have shown how the thermal instability of a conduction channel in SiO_2 thin film, when subjected to high electric fields, can lead to initiation of a dielectric breakdown event. On the basis of this analogy, it can be assumed that the thermal instability of a MIV conduction channel will result from the onset of two processes that can significantly enhance electron emission from the substrate to the electron conduction channel: (i) dissociation of neutral components of impurities (Ridley 1975) and (ii) electron impact ionization (DiStefano and Shatzkes 1976). As will be explained later, both lead to enhancement of the positive ion cloud facing the metallic substrate and, as a result, increase the local field at the surface of the substrate and thus the injection current.

The dissociation model (Ridley 1975) assumes that a large number of neutral components of impurities exist in the conduction channel that have threshold activation energies of dissociation. These components will therefore be dissociated if an external source of energy higher than the threshold is provided. This energy will be available when field emission from the conduction channel occurs, since an electron emission current generates Joule heating when it flows through the channel. With increasing gap field, this current increases and becomes large enough to cause a temperature rise in the channel of, say, 300 °C. It has been shown in a calculation (Xu and Latham 1994) that, typically, a 15 μA current passing through a 5 nm diameter channel will give rise to a 300 °C temperature rise. In this context, it should be noted that a current of about 15 μA is often measured from a single emission site at a typical gap field of 20 MV m^{-1}.

On the other hand, it has been shown independently (Kuhn and Silversmith 1971) that a temperature rise of about 300 °C can activate dissociation of the neutrals, and that this signals the beginning of a significant increase of ion concentration in the channel. These ions will be accelerated towards the MI interface, and produce an extra field E_i. In fact, Xu and Latham (1994) have demonstrated that, if the area density of ions becomes high enough, say, 10^{17} m^{-2}, then the ionic field E_i can be calculated to be equal to 3.6×10^8 V m^{-1}. This is then much higher than the applied fields used in the present study, which are < 30 MV m^{-1}. Under these circumstances, there will be a significant increase in the electron current injected into the conduction channel. This will then result in further Joule heating. Xu and Latham (1994) have further demonstrated that, under these conditions, the temperature rise in a 5 nm diameter channel in a typical dielectric inclusion, such as that shown in figure 6(*a*), is about 10^4 °C.

The electron impact ionization model (DiStefano and Shatzkes 1976) assumes that the ion density required for enhancing the electron emission from the substrate is produced by hot-electron impact ionization. If this impact ionization occurs, electrons are swept towards the vacuum interface, leaving behind a positive cloud, due to the difference in mobility between the electrons and holes. In our case, electrons tunnelling into the conduction channel can gain energy from the very high field at the interface region (see figure 6(*b*)) before being thermalized. However, this field will need to be high if

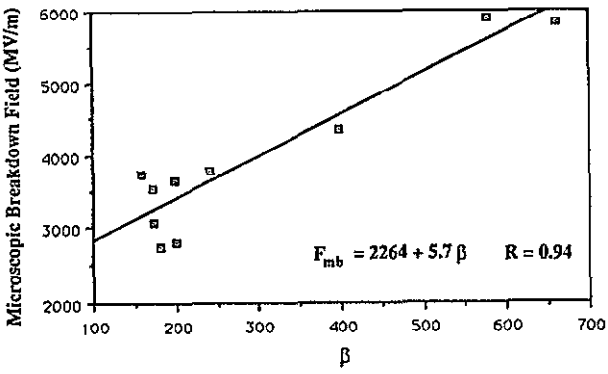

Figure 7. How the microscopic breakdown field $E_{mb}(\beta E_b)$ increases with β.

a conduction electron is to have sufficient kinetic energy to cause a typical band-to-band impact ionization. In summary, we expect that the dissociation process will occur before this field is reached at the MI interface. Therefore, it is believed that the dissociation-induced breakdown process is predominant in the proposed emission regime.

3.2. The dependence of the breakdown field on β

Figure 3 demonstrates how the macroscopic breakdown field of a HV gap decreases with increasing β. It is more important, however, to find out how the locally enhanced microscopic breakdown field acting at a pre-breakdown emission site E_{mb} (defined as βE_b) varies with β. To answer this question, a computer procedure using a Macintosh Cricket Graph program was employed to obtain the microscopic breakdown field E_{mb} as a function of β. As shown in figure 7, this analysis has shown that E_{mb} can be approximated by a simple straight line function having a coefficient of variation of 0.94

$$E_{mb} = 5.7\beta + 2264 \qquad (1)$$

This plot, in conjunction with equation (1), highlights the important new finding that the microscopic breakdown field of an emission site increases with increasing β of the site.

To explain the physical basis of the relationship between E_{mb} and β defined by equation (1), one may imagine the electron conduction channel shown in figure 6(*a*) as an embedded 'metallic' filament in the dielectric medium, similar to the approach of Hurley (1979). Accordingly, the field enhancement factor β will depend upon both the topographic detail of an emitting site and the electronic properties of the conduction channel. In general however, an emitting site having high β will be characterized by having a more metallic-like conduction channel. It follows therefore that, under the same gap field conditions, a 'more metallic' filament will probe the gap field more effectively, and hence promote enhanced emission of electrons, then a 'less metallic' filament. Consequently, a 'more metallic' (high β) emission site is prone to breakdown at lower gap field.

3.3. The relationship between switching-on field and breakdown field

With the exception of the three samples having relatively low β, table 1 shows that the breakdown fields are generally lower than the switching-on fields. This behaviour may be attributed to the establishment of electroformed conduction channels, which are externally manifested as the switching-on process, namely the electroforming process mentioned in section 3.1 As illustrated in figure 6(*b*), a stronger field can appear across the interface between the substrate and the insulating layer after switching-on, and this means that, under such conditions, this interface becomes more likely to be prone to breakdown events.

However, for sites having relatively low β-values, the switching-on process may not cause substantial changes in electronic properties in these channels, that is, it will not increase the conductivity to the point at which they have metallic-like properties. Thus, it is likely that the voltage across the insulating bulk region represents a large part of the total voltage available, so that the voltage across the interface between the substrate and the insulating layer will not increase rapidly. It follows therefore that these sites will have breakdown fields that are higher than the switch-on fields.

3.4. Knock-on effects

Apart from explaining how a PES can become unstable and initiate a breakdown discharge, it is also necessary to give an account of the subsequent time evolution of the extended breakdown process shown in figures 4(*b*) and 5. It can be seen that this involves the successive 'striking' of a sequence of 'secondary' discharges, whose locations occur randomly over the electrode surface. Although these discharge events were all recorded in the single video frame during the opening period of aperture exposure of the video camera, it is believed that the associated sequence of gap voltage collapses recorded in figure 5 strongly points to successive striking of individually localized discharges, such as those displayed in frame 2 of figure 4(*b*). One can therefore imagine that, if the process had been recorded with a camera system that had a higher time resolution, then the integrated events recorded in frames 1 and 2 of figure 4(*b*) would in reality appear as illustrated schematically in figure 8.

As briefly mentioned in section 2.3.3, this 'hopping' of discharge centres during an extended breakdown process may be a consequence of both annihilation of the emission sites that initiate a breakdown and creation of new emission sites. We have already pointed out in section 3.1 that initiation of a breakdown discharge is associated with destruction of a PES. This will result in spreading of droplets of cathode material on the surface of electrodes (Bayliss 1984), where the locations of these droplets can then form new emission sites (Latham *et al* 1986). The findings from this study, as represented by figures 4 and 5, further indicate that these new sites immediately become unstable once the gap field

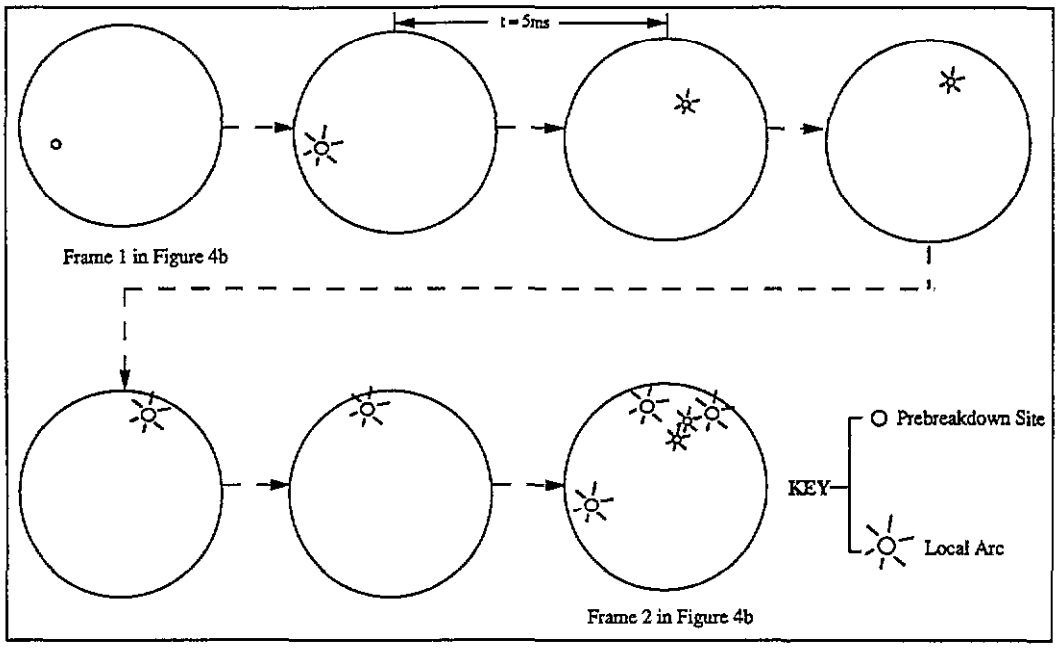

Figure 8. How a breakdown discharge initiated at a pre-breakdown emission site might evolve into a sequential multi-discharge process.

reaches the level of the onset breakdown field. This reasoning also explains the extensive spatial spread of micro-craters observed by previous authors (Schwirzke 1991, Latham and Braun 1970). It follows that one should wonder whether the motion of the cathode spots of a vacuum arc has a physical origin similar to that described above. However, it is not clear at this stage how these sites are triggered sequentially to produce the hopping characteristics of a breakdown event.

4. Conclusions

The following conclusions can be derived from the present study.

(i) A 'primary' breakdown discharge can trigger an extended breakdown event consisting of a sequence of localized and spatially random 'secondary' discharge events.

(ii) A spatial correlation exists between a pre-breakdown emission site and the primary localized discharge of an extended breakdown event.

(iii) In general emission sites with higher β values have lower breakdown gap fields. This behaviour has been explained in terms of these being a more effective enhancement of the local field in the case of high-β sites.

(iv) The microscopic breakdown field, and consequently the critical current density, increases with β. This is explained in terms of the electronic properties of a conduction channel on Joule heating.

(v) 70% of samples have breakdown fields that are lower than the switch-on fields of their emission sites. This is attributed to the change in their electronic properties brought about by the switching-on process.

(vi) The other 30% of samples, having higher breakdown fields, are believed to have sites exhibiting high resistivities in the bulk of the conduction channels, and thus a smaller proportion of the total available voltage is dropped across the interface between the substrate and the insulation region. It follows that samples with such sites can sustain much higher hold-off fields.

Finally, our discussion indicates that the electronic properties of a conduction channel, as well as the two associated interfaces, can have a strong influence on breakdown field level. Thus, electrode treatment procedures, such as thermal processing (Niedermann *et al* 1986), may be designed to modify these properties in order to raise the hold-off capability.

Acknowledgments

This work was supported by the Strategic Defense Initiative Organization's Office of Innovative Science and Technology (SDIO/TIN) through contract number N60921-91-C-0078 with the Naval Surface Warfare Center. The authors also wish to express their appreciation to Professor B M Mazurek for helpful discussions during this investigation.

References

Allen N K and Latham R V 1978 *J. Phys. D: Appl. Phys.* **11** L55–7

Athwal C S and Latham R V 1981 *Physica* C **104** 46–9

Bayliss K H 1984 The physical origin of prebreakdown electron emission from broad-area high voltage electrodes *PhD Thesis* Aston University

Bayliss K H and Latham R V 1986 *Proc. R. Soc.* A **403** 285–311
DiStefano T H and Shatzkes M 1976 *J. Vac. Sci. Technol.* **13** 50–4
Hurley R E 1979 *J. Phys. D: Appl. Phys.* **12** 2247–52
Kuhn M and Silversmith D J 1971 *J. Electrochem. Soc.* **118** 966–9
Lafferty J M 1966 *Proc. IEEE* **54** 23–32
Latham R V 1981 *HV Vacuum Insulation: The Physical Basis* (London: Academic)
—— 1988 *IEEE Trans. Electr. Insul.* **23** 881–94
Latham R V, Bayliss K H and Cox B M 1986 *J. Phys. D: Appl. Phys.* **19** 214–31
Latham R V and Braun E 1970 *J. Phys. D: Appl. Phys.* **3** 1663–9
Latham R V and Xu V S 1991 *Vacuum* **42** 1173–81
Mesyates G A and Proskurovsky D I 1989 *Pulsed Electrical Discharge in Vacuum* (Berlin: Springer) p 79
Niedermann Ph 1986 Experiments on enhanced field emission *PhD Thesis* University of Geneva
Niedermann Ph, Sankarraman N, Noer R J and Fischer Ø 1986 *J. Appl. Phys.* **59** 892–7
Ridley B K 1975 *J. Appl. Phys.* **46** 998–1007
Schwirzke F R 1991 *IEEE Trans. Plasma Sci.* **19** 690–6
Solomon P 1977 *J. Vac. Sci. Technol.* **14** 1122–30
Xu N S 1986 Field-induced hot-electron emission from composite metal–insulator–metal microstructures *PhD Thesis* Aston University
Xu N S and Latham R V 1995 *High Voltage Vacuum Insulation, Basic Concepts and Technological Practice* (London: Academic) ch 5 to be published